

Nanoscale

Accepted Manuscript



This is an *Accepted Manuscript*, which has been through the Royal Society of Chemistry peer review process and has been accepted for publication.

Accepted Manuscripts are published online shortly after acceptance, before technical editing, formatting and proof reading. Using this free service, authors can make their results available to the community, in citable form, before we publish the edited article. We will replace this *Accepted Manuscript* with the edited and formatted *Advance Article* as soon as it is available.

You can find more information about *Accepted Manuscripts* in the [Information for Authors](#).

Please note that technical editing may introduce minor changes to the text and/or graphics, which may alter content. The journal's standard [Terms & Conditions](#) and the [Ethical guidelines](#) still apply. In no event shall the Royal Society of Chemistry be held responsible for any errors or omissions in this *Accepted Manuscript* or any consequences arising from the use of any information it contains.

ARTICLE

Injectable small molecule hydrogel as a potential nanocarrier for localized and sustained *in vivo* delivery of Doxorubicin

Cite this: DOI: 10.1039/x0xx00000x

Manish Singh,^{a,†} Somanath Kundu,^{a,†} Amarendar Reddy M,^{b,†} Vedagopuram Sreekanth,^a Rajender K. Motiani,^c Sagar Sengupta,^{d,*} Aasheesh Srivastava,^{b,*} and Avinash Bajaj^{a,*}Received 00th January 2012,
Accepted 00th January 2012

DOI: 10.1039/x0xx00000x

www.rsc.org/

Majority of localized drug delivery systems are based on polymeric or polypeptide scaffolds, as weak intermolecular interactions of low molecular weight hydrogelators (LMHGs, MW <500 Da) are significantly perturbed in presence of anticancer drugs. Here, we present *L*-alanine derived low molecular weight hydrogelators (LMHGs) that remain injectable even after entrapping anticancer drug doxorubicin (DOX). These DOX containing nanoassemblies (DOX-Gel) showed promising anticancer activity in mice models. Subcutaneous injection of DOX-Gel near tumor achieved greater decrease in tumour load than intravenous injection of DOX (DOX-IV), and local injection of DOX alone (DOX-Local) at tumor site. We noticed that DOX-Gel nanocarriers are especially effective when injected during early stage of tumor progression, and achieve substantial decrease in tumor load in long term.

Introduction: Efficacy of cancer chemotherapy is limited by systemic and cellular transport mechanisms of our body as most of drugs are administered orally or *via* intravenous routes.¹ Administration of chemotherapeutics faces multiple challenges before they can act at the site of disease.² Many pharmaceuticals fall short of realizing their potential due to their poor bioavailability, high toxicity, short plasma half-life, low permeability across cell membrane, and rapid clearance from body.³ To overcome these impediments, advanced drug delivery systems based on liposomes,⁴ polymers,⁵ and gold nanoparticles⁶ have been engineered and explored for drug delivery.⁷ These delivery systems are often non-discriminating, and deliver anticancer drugs to healthy tissues with detrimental effects.⁸ Therefore, there is an urgent need for localized drug delivery vehicles that would have beneficial characteristics of improved efficacy, reduced toxicity, and sustained drug release with minimal side effects.⁹

Doxorubicin (DOX) is a potent anticancer drug that inhibits cancer cell growth by intercalating between DNA base pairs and inducing DNA breaks.¹⁰ Liposomal formulations of DOX like Doxil, Caleyx, and Myocet are commercial available and used for treatment of cancer.¹¹ Accumulation of DOX enhances risk of developing cardiomyopathy, cardiac dilatation, and heart failure even with liposomal formulations.¹² Therefore, development of strategies aimed at sustained localized delivery of DOX is required for proficient cancer treatment.

Localized drug delivery involves use of implantable or injectable systems with sustained drug release characteristics that would prevent growth of cancerous cells which cannot be removed during resection.¹³ Polymeric hydrogels¹⁴ and low molecular weight hydrogelators (LMHGs)¹⁵ capable of self-assembly are being investigated for localized drug delivery in cancer.¹⁶ Self-assembling nanocarriers based on LMHGs open up new avenues for chemists to design efficient delivery agents whose release-profiles could be altered by chemical and/or physical stimuli.¹⁷ LMHGs have additional advantages over their polymeric counterparts like lower cytotoxicity, lesser immunogenicity, predictable degradation pathways, and formation of networks like ECM.¹⁸ Similarly, synthetic derivatives of some anticancer drugs have shown self-assembly propensity, and have been explored for drug delivery.¹⁹ However, since intermolecular forces holding these molecular assemblies are often weak, they can readily fall apart in presence of shear forces encountered during drug encapsulation or injection through syringe.²⁰ LMHGs often show thixotropic (shear-thinning) behavior.²⁰ However, for most LMHGs, once the self-assembled fibrillar networks disintegrate due to shear, their re-construction may be a slow process, requiring hours to complete. This slow recovery of gel-strength is undesirable for *in vivo* applications.

Herein, we present low molecular weight derivatives of *L*-alanine to exemplify a new paradigm in development of injectable localized drug delivery agents. These derivatives, each with molecular weight of <300 Da, undergo self-assembly in aqueous medium through inter-molecular hydrogen bonding. We demonstrate that these compounds can readily entrap DOX, and still form injectable assemblies (Fig. 1). These drug-carrying hydrogels were then explored for tumor regression studies using *in vivo* mice models.

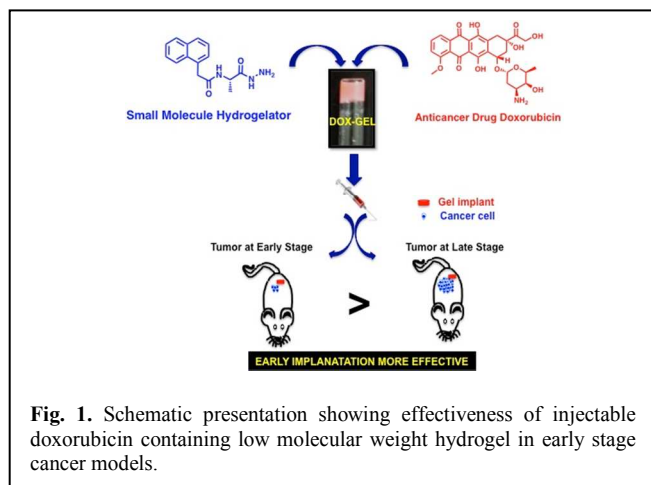


Fig. 1. Schematic presentation showing effectiveness of injectable doxorubicin containing low molecular weight hydrogel in early stage cancer models.

Results and Discussion: As amino acid is common feature in many hydrogelators,²¹ molecular feature of these gelators is presence of an aromatic *N*-protecting group on *L*-alanine that is designed to be rotationally flexible (Fig. 2a). Use of such rotationally-flexible aromatic residues accentuates nanofiber formation. Hydrogen-bonding elements in these compounds were augmented by addition of carboxamide or hydrazide units at carboxylic end of alanine. A protonated variant of **ALA-HYD** was also prepared in the form of **ALA-HYD+** with chloride counter ion (Fig. 2a, Scheme 1, ESI). Initial cytotoxicity studies confirmed that all these alanine derivatives are non-toxic to cancer cells on their own (Fig. S1, ESI). Gelation studies showed that upon cooling hot sols, all three molecules could rigidify water at ambient conditions. Minimum gelation concentration (MGC) for all these molecules was $\leq 1.0\%$ w/v (Fig. 2b). Atomic force micrographs of resulting assemblies showed each xerogel composed of nanofibers (for **ALA-CAM**, **ALA-HYD**) (Fig. 2c, d) or a combination of globules and nanofibers for **ALA-HYD+** (Fig. 2e). We confirmed nanofiber structures of **ALA-HYD** hydrogels (Fig. S2a, ESI); and globular nature of **ALA-HYD+** hydrogels (Fig. S2b, ESI) by SEM studies; whereas **ALA-CAM** hydrogels were unstable in SEM conditions. These nano-assemblies are thermally robust up to 58 ± 2 °C, as confirmed by invert-vial experiments. Rheology studies showed that even at MGC, resulting gels were mechanically strong, with storage modulus (G') values being in range of 10^6 Pa (Fig. S3a-b, ESI). **ALA-CAM** gave materials with highest G' values, reflecting stronger intermolecular hydrogen bonding by carboxamide unit that is sterically least encumbered (Fig. S3a-b, ESI). Hydrogels formed by hydrazide compounds (**ALA-HYD** and **ALA-**

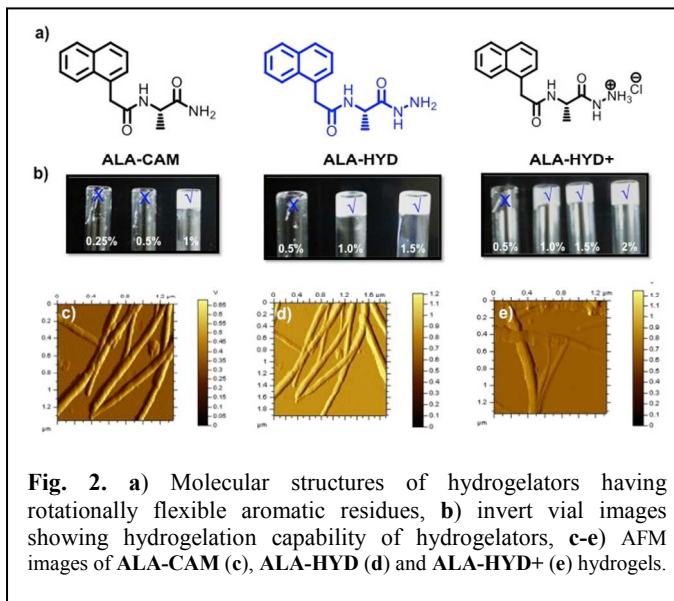


Fig. 2. a) Molecular structures of hydrogelators having rotationally flexible aromatic residues, b) invert vial images showing hydrogelation capability of hydrogelators, c-e) AFM images of **ALA-CAM** (c), **ALA-HYD** (d) and **ALA-HYD+** (e) hydrogels.

HYD+) were only slightly weaker with G' value $\sim 10^5$ Pa. Therefore, all derivatives turned out to be rather strong hydrogelators at $>1\%$ (w/v) concentrations.

We then attempted physical entrapment of anticancer drug doxorubicin (DOX) during formation of these hydrogels. DOX solution was added to hot aqueous sol of gelator, and resulting mixture was allowed to cool naturally under ambient conditions. We observed that carboxamide analogue **ALA-CAM** could not form stable gels with DOX (Fig. 3a-b), whereas hydrazide derivatives (**ALA-HYD** and **ALA-HYD+**) form stable hydrogels even in presence of DOX (Fig. 3a/b). Introduction of hydrazide functionality in these molecules ensured facile encapsulation of DOX at 40 and 80 $\mu\text{g}/200$ μL concentration (Fig. 3a, b). **ALA-HYD** and **ALA-HYD+** could encapsulate **DOX** at ≥ 1.5 and $\geq 2.0\%$ gelator concentration to yield stable hydrogels. At lower gelator concentrations, resulting gels were mechanically weaker. Gels prepared from

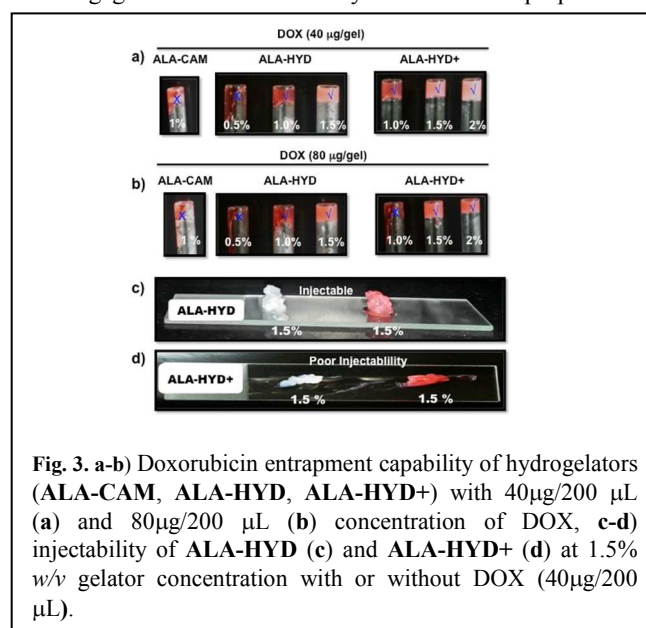
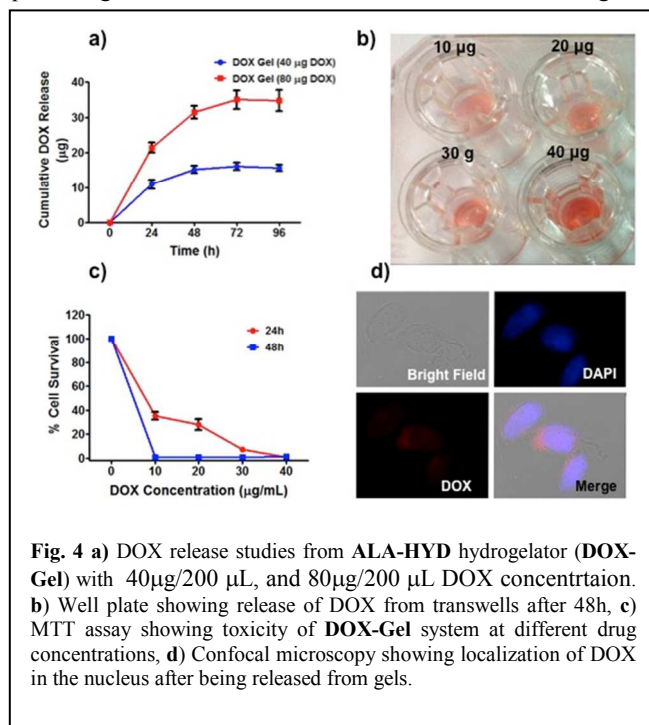


Fig. 3. a-b) Doxorubicin entrapment capability of hydrogelators (**ALA-CAM**, **ALA-HYD**, **ALA-HYD+**) with 40 $\mu\text{g}/200$ μL (a) and 80 $\mu\text{g}/200$ μL (b) concentration of DOX, c-d) injectability of **ALA-HYD** (c) and **ALA-HYD+** (d) at 1.5% w/v gelator concentration with or without DOX (40 $\mu\text{g}/200$ μL).

ALA-HYD were readily injectable through a 20 gauge syringe in their pristine as well as in its DOX encapsulating state (Fig. 3c), whereas **ALA-HYD**+ gel with DOX had poor injectability (Fig. 3d). Gels prepared from **ALA-CAM** were mechanically disintegrated upon passing through syringe (not shown).

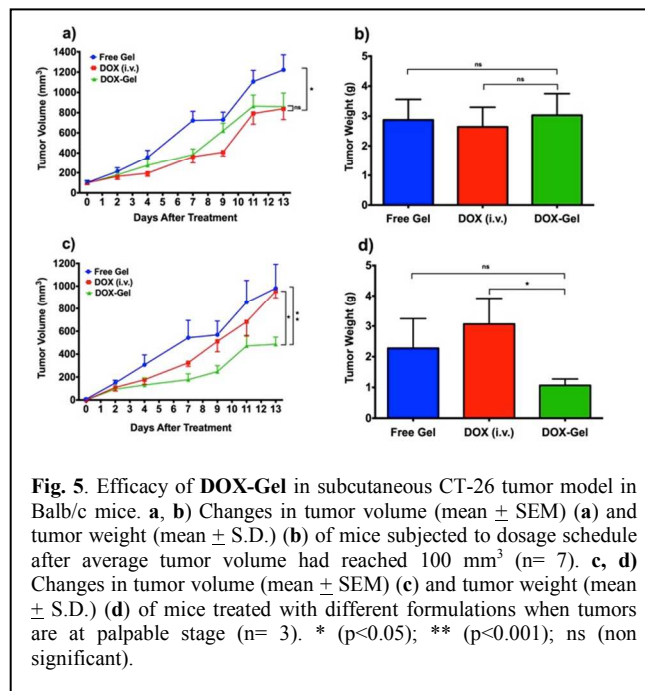
Above studies suggested that **ALA-HYD** gelator is most robust gelator with high mechanical strength, and good injectability. Further investigations were thus focused on this compound. Time dependent rheological studies on gels formed by **ALA-HYD** confirmed their thixotropic behavior (Figure S3c, ESI) confirming rapid recovery of gel-strength upon removal of shear stress. Within 5 min of removal of stress, gel-strength was similar to pristine gel-strength. Rheological studies further established stability of **ALA-HYD** gels at physiologically relevant conditions (37 °C, pH 7.4); and acidic pH 5.8 (Fig. S3d-3e, ESI). Scanning electron microscopy (SEM) imaging of **ALA-HYD** xerogels revealed similar self-assembled fibrillar nanoassemblies as observed in pristine xerogels (Fig. S4a-b, ESI). Rheology studies of **ALA-HYD** showed no perceptible change in mechanical strength upon DOX encapsulation (Fig. S4c, ESI). Hydrogel formed by **ALA-HYD** showed a T_m value of 58 ± 2 °C, and this value did not change even after DOX entrapment. Therefore, entrapment of DOX had virtually no influence on morphology, thermal, and mechanical stability of **ALA-HYD** gels.

We then investigated whether DOX is physically entrapped within the gel framework or is having any chemical interaction with gelator molecules. Fluorescence titration studies showed quenching of DOX fluorescence on titrations with gelator



ALA-HYD molecules (Fig. S4d, ESI). MALDI studies of DOX entrapped gel revealed formation of covalent imine bond between free amine of gelator and carbonyl group of DOX (Fig. S4e, ESI). Imine bond between **ALA-HYD** and DOX is

reversible and can be cleaved in vicinity of tumors. This would allow sustained release of DOX.



We then studied drug release profile of these DOX encapsulated **ALA-HYD** hydrogels (**DOX-Gel**) in PBS (pH 7.4) at 37 °C. We observed that **DOX-Gel** system indeed allowed slow and sustained release of DOX, with only ~40% of entrapped drug released at 96 h (Fig. 4a). We then studied cytotoxicity of this **DOX-Gel** system against 4T1 cells using transwells (Fig. 4b). MTT assay²² concluded that **DOX-Gel** induces cellular toxicity after 24h and 48h (Fig. 4c). Confocal microscopy studies confirmed co-localization of DOX in nuclear compartment (Fig. 4d, Fig. S5, ESI) suggesting the cellular uptake of DOX is responsible for cellular toxicity.

In order to explore *in vivo* anticancer potential of **DOX-Gel**, we used two different tumor (Colon and Breast) model systems. We initially developed colon tumors by injecting CT-26 cells in Balb/c mice.²³ To explore efficacy of **DOX-Gel** in early and late stage tumors, we divided mice into two groups: one mice group bearing palpable tumors, and another mice group bearing developed tumors (~100 mm³). **DOX-Gel** was injected subcutaneously in vicinity of tumor. Gel alone without DOX, (**Free Gel**), and intravenous injection of DOX (**DOX-IV**) was employed as controls. We observed ~25% reduction in tumor volume with **DOX-IV**, and **DOX-Gel** as compared to **Free Gel** control group in mice where tumor was at developed stage (Fig. 5a). There was no significant difference in tumor volume and tumor weight between **DOX-Gel** and **DOX-IV** treatment groups (Fig. 5a, 5b). In contrast, we observed ~20% reduction in tumor volume (Fig. 5c) and ~60% decrease in tumor weight (Fig. 5d) on **DOX-Gel** treatment as compared to **DOX-IV** and **Free Gel** in mice with palpable tumors. These results suggested that **DOX-Gel** treatment is more effective than **DOX-IV** in mice with early stage tumors. High potency of **DOX-Gel** might

be due to slow and localized release of **DOX** from **DOX-Gel**, whereas **DOX-IV** was in circulation and may require multiple doses that carry associated risk of cardiotoxicity.

To further validate efficacy of **DOX-Gel**, we conducted *in vivo* experiments using breast tumor model by injecting 4T1 cells in Balb/c mice²⁴ and investigated the potential of **DOX-Gel** in early stage tumors for long duration. After 2 days of cell injection, mice were divided into four groups of 8-10 mice in each set and were treated with a) untreated control, b) **Free Gel**, c) **DOX-IV**, and d) **DOX-Gel**. Single implantation of **DOX-Gel** reduces tumor volume by ~50% (Fig. 6a) as compared to untreated control on 11th day. Implantation of **Free Gel** did not cause any change in tumor volume. We sacrificed 3 mice in each group at 11th day to measure the changes in tumor weight, and to explore the mechanism of tumor regression; and followed rest of mice. We observed 4-fold and 2-fold reduction in tumor weight by **DOX-Gel** as compared to control and **DOX (IV)** treated mice respectively (Fig. 6b, c). Prolonged observations of mice suggested diminished effect of **DOX (IV)** as tumors grew at a similar rate to those observed for **Free Gel** treated mice, whereas **DOX-Gel** reduced tumor volume by 40% as compared to **DOX (IV)** (Fig. 6d) without much change in body weight of mice (Fig. S6, SI).

We then studied mechanism of tumor regression in tumors harvested from mice by performing western blotting for apoptotic markers. Treatment of **DOX-Gel** induces cleavage of caspase-7, -3 and -8, as observed in western blot studies (Fig. 7a), indicating activation of apoptotic pathway responsible for tumor regression. Tunnel assay on tumor tissues confirmed apoptotic mechanism of tumor regression by **DOX-Gel** as we observed high number of apoptotic Tunnel-positive cells showing DNA breaks in **DOX-Gel** treated mice (Fig. 7d) as compared to control and **DOX (IV)** treated tissues (Fig. 7c).

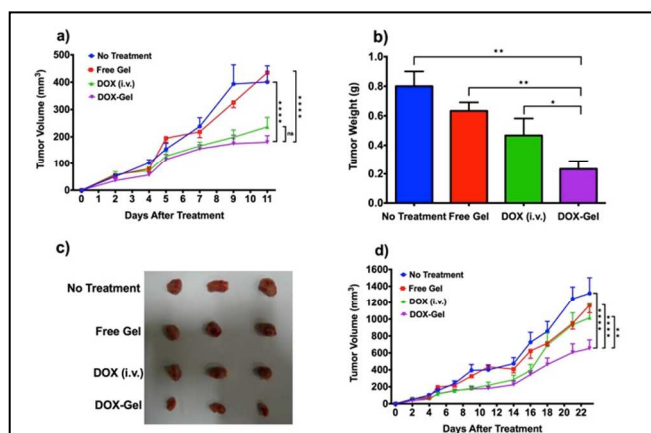


Fig. 6. Efficacy of **DOX-Gel** formulation in subcutaneous 4T1 murine breast tumor model in Balb/c mice. **a)** Change in tumor volumes (mean \pm SEM) of mice treated with formulations at stage of palpable tumors (n= 10) up to day 11; **b)** Change in the tumor weight (gm.) of tumors excised (mean \pm S.D.) from mice (n= 3) on day 11; **c)** Representative excised tumor pictures of No Treatment, **Free Gel**, **DOX (IV)**, and **DOX-Gel** group mice (n= 3); **d)** Change in tumor volume (mean \pm SEM) of mice treated with formulations at stage of palpable tumors up to day 23 (n= 7 from day 11). * (p<0.05); ** (p<0.001); **** (p<0.0001); ns (non significant).

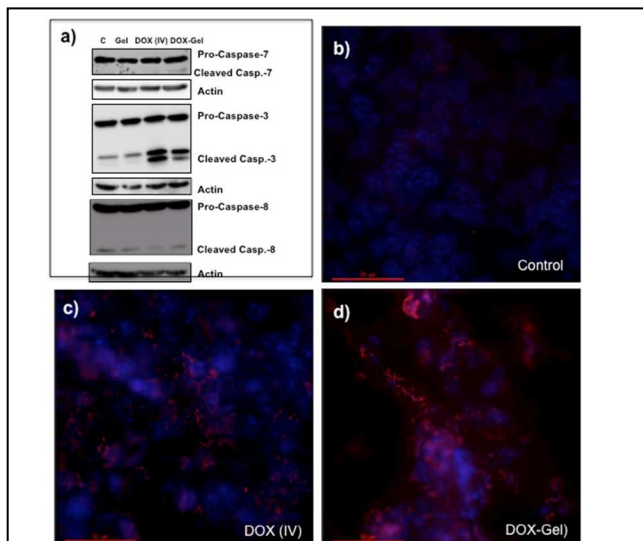


Fig. 7. a) Western blot of tumors showing presence of cleaved caspase indicating **DOX** mediated apoptosis; **b-d)** Tunnel assay of tumor samples **b)** control, **c)** **DOX (IV)**, and **DOX-Gel** treatment showing high apoptosis by **DOX-Gel**.

We then compared *in vivo* potential of **DOX-Gel** with mice group, where we injected equivalent dose of **DOX** locally (**DOX-Local**) to compare antitumor efficacy of **DOX-Gel** with one-time localized delivery of active drug. We observed that effect of **DOX-Local** gets totally diminished, whereas **DOX-Gel** reduces tumor burden by ~40% as compared to untreated control (Fig. 8a, b). Therefore, *in vivo* tumor regression studies confirmed that **DOX-Gel** is able to regress tumor progression in mice for a significantly longer duration due to slow and sustained release of **DOX**, whereas **DOX-Local** is not effective for tumor regression due to its high diffusion.

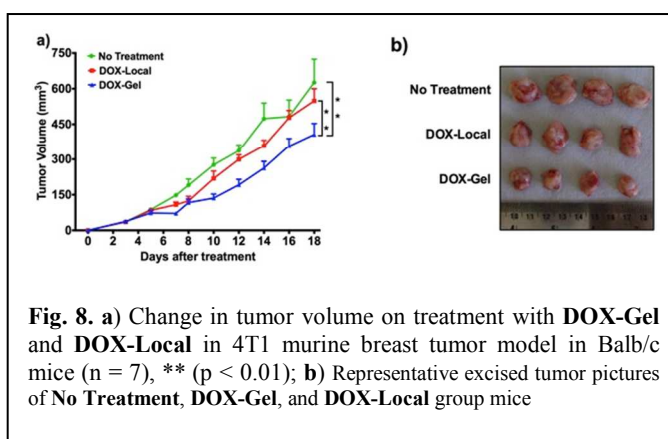


Fig. 8. a) Change in tumor volume on treatment with **DOX-Gel** and **DOX-Local** in 4T1 murine breast tumor model in Balb/c mice (n = 7), ** (p < 0.01); **b)** Representative excised tumor pictures of No Treatment, **DOX-Gel**, and **DOX-Local** group mice

We then performed pharmacokinetic studies to quantify **DOX** in blood at different time points on treatment with **DOX-Gel**, **DOX (IV)**, and **DOX-Local** in tumor bearing mice. We have not observed any **DOX** presence in blood serum after 2, 6, 24, and 72h in treated mice. We believe that absence of **DOX** in blood might be due to very low amounts of **DOX** released in the blood, which is beyond the detection limits of our assay. It is to be noted that we have used only 40 μ g of **DOX** per mice

(~2 mg/kg) for our studies as compared to high toxic dose of ~30 mg/kg used for polymeric hydrogel based *in vivo* mice studies.²⁵

Conclusions: In summary, we report small molecular hydrogelators that form injectable hydrogels even after encapsulating anticancer drugs like doxorubicin (DOX). We noticed that DOX is covalently attached with gelator through imine bond, which is known to be unstable under acidic conditions found in vicinity of tumors. The DOX-containing gels were able to regress tumor load at palpable stage when injected at site of tumors. We believe that slow release of DOX caused higher reduction in tumor burden in tumor models at their early stages. We hope that this study would draw attention of researchers in designing of new LMHGs for localized anticancer therapy.

Experimental Section

In vitro Dox release: A weighted amount of DOX (40/80 μg) per 200 μL of 1.5% of hydrogelator was casted in upper chamber above polycarbonate membrane (0.4 μm) of transwell plate and 800 μL of PBS (pH 7.4) solution was taken in lower compartment of transwell plate. During experiments, plate was kept at 37 °C, in a humidified atmosphere. At desired time point (24, 48, 72 and 96 h) transwell was transferred to well having fresh PBS solution. Amount of DOX released in lower compartment of plate was calculated by measuring doxorubicin fluorescent intensity (Excitation 480 nm/Emission 560 nm). Cumulative DOX release was plotted by converting fluorescent intensity to corresponding DOX concentration. All experiments were done in triplicates.

Cell viability tests: Mouse mammary gland cancer cell line 4T1 was cultured in RPMI 1640 medium (Sigma-Aldrich), supplemented with 10% fetal bovine serum (FBS; Sigma-Aldrich), 1% (v/v) Pen-Strep, at 37 °C, under 5% CO₂ in a humidified atmosphere. We seeded ~1 × 10⁴ cells per well in lower compartment of 24 well of corning transwell plate. Cells were seeded 1 day before experiments for proper attachment of cells and each well having 800 μL of complete growth media. DOX (10, 20, 30 & 40 μg/mL) loaded gel was casted in transwell filter and at desired end point of experiment cytotoxicity by DOX diffusion from upper chamber was evaluated by MTT assay. Light absorbance was measured at 555 nm wavelength using a micro plate reader. Similarly, toxicity of gelator molecules at different conditions was performed in 96-well plate using previous procedures.²⁶

CT-26 murine colon cancer model: Animals were maintained using standard protocols at Animal facility, NII, New Delhi. All animal experiments were done with approval of Institutional Animal Ethical Committee (IAEC), NII, New Delhi. CT-26 murine colon cancer cells (1.5 × 10⁶) in 100 μL matrigel were implanted sub-cutaneously into right flanks of 6 weeks old female Balb/C mice using 20 gauge needle. For treatment, mice were divided into two groups one bearing tumour volume upto 100 mm³ having randomised into following groups a) Free Gel, b) DOX (IV) (40 μg/ 200 μL), and c) DOX-Gel (40 μg/200 μL) (n=7) and palpable group categorised into three groups as a) Free Gel, b) DOX (IV), and c) DOX-Gel (n = 3).

4T1 murine breast cancer model: 4T1 murine mammary carcinoma cells (1.5 × 10⁶) in 100 μL matrigel were injected sub-cutaneously

into right flanks of 6 weeks old female Balb/C mice. After two days, mice were randomised into 4 groups a) no treatment group, b) free gel, c) DOX (IV) injected group (40 μg/200 μL) and d) DOX-Gel (40 μg/200 μL) injected group. Free gel without DOX and DOX-Gel were both injected subcutaneously near the vicinity of tumour using 20 gauge needle. Doxorubicin was given intravenously through lateral tail vein. Only a single dose was given throughout study period. Similarly, similar amount of doxorubicin was given locally. Tumour volume was measured every alternate day with a digital caliper using formula $L \times B^2 / 2$ followed by continuous monitoring of body weight.

Western blotting: For protein isolation, a slice of tumour was cut with a scalpel blade from each tumour sets. Cut tissues were then homogenised in homogenization tubes containing RIPA buffer with protease and phosphatase inhibitor cocktail (Sigma) in a mechanised homogenizer (Precellys lysis and homogenization platform). Homogenised samples were subjected to sonication for 5 minutes at 4 °C. Samples were then centrifuged at 16,000xg at 4 °C for 10 minutes. Soluble protein in supernatant was collected. Protein estimation was done using the CB-XTM protein estimation kit (G-biosciences). 30 μg of protein was loaded in to the each lane of 10% poly-acrylamide gel to run SDS-PAGE. Protein was transferred to 0.2 μm pore size PVDF membrane (MDI, Ambala) following wet transfer method. 5% skimmed milk was used for blocking membrane for non-specific antibody binding. 1:2000 dilutions of antibodies Caspase 3, Caspase 7, Caspase 8 (Cell Signalling Technology) in 5% Skimmed milk in PBST were used. Membranes were incubated with primary antibodies overnight at 4 °C. A dilution of 1:5000 was used for secondary anti-rabbit (Cell Signalling Technology). For Chemiluminescence detection equal amount of luminal substrate and hydrogen peroxide were used (ECL Kit Amersham). Blots were re-probed with β-actin antibody.

TUNEL Assay: 6-8 μm thick tumour sections were cut out of cryopreserved OCT embedded blocks and placed over Poly-L-lysine coated slides (Sigma). To find out apoptotic cells in treated samples terminal deoxynucleotidyl transferase-mediated dUTP nick end labelling (TUNEL) reaction was performed using kit (In Situ Cell Death detection Kit, TMR red, Roche) following manufacturers instructions. Image acquisition was done using a fluorescent microscope (GE-API-DV-Elite inverted fluorescent microscope) in 60x magnification in oil immersion. All images were deconvoluted after image acquisition using deconvolution software.

Supporting Information:

Electronic Supplementary Information (ESI) available: [Scheme 1, Figures S1-S6, synthesis of hydrogels; experimental section for gelation, rheology, MALDI, microscopy and pharmacokinetic studies]. See DOI: 10.1039/b000000x/

Acknowledgements

We thank RCB, IISER, NII for intramural funding and Department of Biotechnology, Govt. of India for funding. AB thanks DST for Ramanujan fellowship. SK and VS thank RCB for fellowships. ARM thanks IISER Bhopal for institute fellowship. AB thanks DST for Ramanujan fellowship.

Notes and references

a: Laboratory of Nanotechnology and Chemical Biology, Regional Centre for Biotechnology, 180 Udyog Vihar, Phase 1, Gurgaon-122016, India. Email: bajaj@rcb.res.in

b: Department of Chemistry, Indian Institute of Science Education and Research, Bhopal, India. Email: asri@iiserb.ac.in

c: Institute of Genomics and Integrative Biology, New Delhi, India.

d: National Institute of Immunology, Aruna Asif Ali Marg, New Delhi, India. Email: sagar@nii.res.in

†Authors contributed equally.

- (a) T. M. Allen, and P. R. Cullis, *Science*, 2004, **303**, 1818. (b) Y. Zheng, H. Fu, M. Zhang, M. Shen M. Zhu, and X. Shi, *Med. Chem. Commun.* 2014, **5**, 879. (c) C. Hess, D. Venetz, and D. Neri, *Med. Chem. Commun.* 2014, **5**, 408. (d) H. Dong, C. Dong, W. Xia, Y. Li, and T. Ren, *Med. Chem. Commun.* 2014, **5**, 147.
- (a) K. Riehemann, S. W. Schneider, T. A. Luger, B. Godin, M. Ferrari, and H. Fuchs, *Angew. Chem. Int. Ed.*, 2009, **48**, 872. (b) J. Jin, W. Sirl Lee, K. M. Joo, K. K. Maiti, G. Biswas, W. Kim, K. Kim, S. J. Lee, K. Kim, D. Nam, and S. Chung, *Med. Chem. Commun.*, 2011, **2**, 270. (c) J. Im, S. Kim, Y. Jeong, W. Kim, D. Lee, W. Sirl Lee, Y. Chang, K. Kim, and S. Chung, *Med. Chem. Commun.*, 2013, **4**, 310.
- (a) H. Rosen, and T. Abribat, *Nat. Rev. Drug Discov.*, 2005, **4**, 381. (b) L. Pollaro, and C. Heinis, *Med. Chem. Commun.*, 2010, **1**, 319.
- (a) V. P. Torchilin, *Nat. Rev. Drug Discov.*, 2005, **4**, 145. (b) H. Dong, C. Dong, Y. Feng, T. Ren, Z. Zhang, L. Li, and Y. Li, *Med. Chem. Commun.*, 2012, **3**, 1555.
- R. Duncan, *Nat. Rev. Cancer*, 2006, **6**, 688.
- (a) L. Zheng, J. Zhu, M. Shen, X. Chen, J. R. Baker, S. H. Wang, G. Zhang, and X. Shi, *Med. Chem. Commun.*, 2013, **4**, 1001. (b) M. Stanley, N. Cattle, J. McCauley, S. R. Martin, A. Rashid, R. A. Field, B. Carbain, and H. Streicher, *Med. Chem. Commun.*, 2012, **3**, 1373. (c) Z. Zhang, J. Jia, Y. Ma, J. Weng, Y. Sun, and L. Sun, *Med. Chem. Commun.*, 2011, **2**, 1079.
- E. Soussan, S. Cassel, M. Blanzat, and I. Rico-Lattes, *Angew. Chem. Int. Ed.*, 2009, **48**, 274.
- (a) M. Ferrai, *Nat. Rev. Cancer*, 2005, **5**, 161. (b) C. Hess, D. Venetz, and D. Neri, *Med. Chem. Commun.*, 2014, **5**, 408. (c) J. F. Arambula, J. L. Sessler, and Z. H. Siddik, *Med. Chem. Commun.*, 2012, **3**, 1275.
- (a) B. D. Weinberg, E. Blanco, and J. Gao, *J. Pharm. Sci.* 2008, **97**, 1681; (b) G. W. Ashley, J. Henise, R. Reid, and D. V. Santi, *Proc. Natl. Acad. Sci. USA*, 2013, **110**, 2318.
- (a) S. Amselem, R. Cohen, S. Druckmann, A. Gabizon, D. Goren, R. M. Abra *et al* *J. Liposome Res.*, 1992, **2**, 93. (b) Li Li, Ming Zhao, Wenhao Li, Yuji Wang, Zhuge Zhang, Ran An and Shiqi Peng *Med. Chem. Commun.*, 2012, **3**, 1059-1061 (c) W. T. Truong, Y. Su, J. T. Meijer, P. Thordarson, and F. Braet, *Chem. Asian J.*, 2011, **6**, 30.
- S. Verma, S. Dent, B. J. W. Chow, D. Rayson, and T. Safra, *Cancer Treatment Rev.*, 2008, **34**, 391.
- D. Jain, *J. Nucl. Cardiol.*, 2000, **7**, 53.
- A. Vashist, A. Vashist, Y. K. Gupta, and S. Ahmad, *J. Mater. Chem., B*, 2014, **2**, 147.
- A. V. Kabanov, and V. S. Vinogradov, *Angew. Chem. Int. Ed.*, 2009, **48**, 5418.
- F. Zhao, M. L. Ma, and B. Xu, *Chem. Soc. Rev.*, 2009, **38**, 883.
- (a) R. Tian, J. Chen, and R. Niu, *Nanoscale* 2014, **6**, 3474, (b) N. T. Qazvini, S. Bolisett, J. Adamick, and R. Mezzenga *Biomacromolecules* 2012, **13**, 2136; (c) J. Nanda, A. Biswas, and A. Banerjee, *Soft Matter*, 2013, **9**, 4198; (d) A. Baral, S. Roy, A. Dehsorkhi, I. W. Hamley, S. Mohapatra, S. Ghosh, and A. Banerjee, *Langmuir* 2014, **30**, 929.
- (a) P. K. Vemula, N. Wiradharma, J. A. Ankrum, O. R. Miranda, G. John, and J. M. Karp, *Curr. Opin. Biotech.*, 2013, **24**, 1174; (b) L. A. Estro, and A. D. Hamilton, *Chem. Rev.*, 2004, **104**, 1201; (c) M. C. Branco, D. J. Pochan, N. J. Wagner and J. P. Schneider, *Biomaterials*, 2010, **31**, 9527; (d) S. Koutsopoulos and S. G. Zhang, *J. Controlled Release*, 2012, **160**, 451.
- (a) R. Lin, A. G. Cheetham, P. Zhang, Y.-a. Lin and H. Cui, *Chem. Commun.*, 2013, **49**, 4968; (b) C. Sinthuvanich, A. S. Veiga, K. Gupta, D. Gaspar, R. Blumenthal, and J. P. Schneider, *J. Am. Chem. Soc.*, 2012, **134**, 6210; (c) M. C. Branco, D. J. Pochan, N. J. Wagner, and J. P. Schneider, *Biomaterials*, 2010, **31**, 9527; (d) J. P. Schneider, D. J. Pochan, B. Ozbas, K. Rajagopal, L. Pakstis, and J. Kretsinger, *J. Am. Chem. Soc.*, 2002, **124**, 15030; (e) K. L. Niece, J. D. Hartgerink, J. J. Donners, and S. I. Stupp, *J. Am. Chem. Soc.*, 2003, **125**, 7146; (f) Y. Zhang, Y. Kuang, Y. Gao, and B. Xu, *Langmuir*, 2011, **27**, 529-537; (g) H. Wang, and Z. Yang, *Soft Matter*, 2012, **8**, 2344. (h) R. Huang, W. Qi., L. Feng, R. Su, and Z. He. *Soft Matter*, 2011, **7**, 6222; (i) P. K. Vemula, J. Li, G. John, *J. Am. Chem. Soc.*, 2006, **128**, 8932; (j) B. Adhikari, and A. Banerjee, *Soft Matter*, 2011, **7**, 9259.
- (a) Y. Gao, Y. Kuang, Z. F. Guo, Z. H. Guo, I. J. Krauss, and B. Xu, *J. Am. Chem. Soc.*, 2009, **131**, 13576; (b) H. M. Wang, C. H. Yang, L. Wang, D. L. Kong, Y. J. Zhang, and Z. M. Yang, *Chem. Commun.*, 2011, **47**, 4439; (c) L. Mao, H. Wang, M. Tan, L. Ou, D. Kong, and Z. Yang, *Chem. Commun.*, 2012, **48**, 395; (d) H. Wang, J. Wei, C. Yang, H. Zhao, D. Li, Z. Yin *et al* *Biomaterials*, 2012, **33**, 5848.
- L. A. Estroff, and A. D. Hamilton, *Chem. Rev.*, 2004, **104**, 1201.
- (a) M. Suzuki, and K. Hanabusa, *Chem. Soc. Rev.*, 2009, **38**, 967; (b) A. Reddy, A. Sharma, and A. Srivastava *Chem. Eur. J.*, 2012, **18**, 7575; (c) A. Reddy, A. Sharma, Q. Maqbool, and A. Srivastava *RSC Advances*, 2013, **3**, 18900.
- M. Singh, A. Singh, S. Kundu, S. Bansal, and A. Bajaj *Biochim. Biophys. Acta.*, 2013, **1828**, 1926.
- J. A. MacKay, M. Chen, J. R. McDaniel, W. Liu, A. J. Simnick, and A. Chilkoti, *Nat. Mater.*, 2009, **8**, 993.
- V. Sreekanth, S. Bansal, R. K. Motiani, S. Kundu, S. K. Muppu, T. D. Majumdar *et al* *Bioconjug. Chem.*, 2013, **18**, 1468.
- A. M. Al-Abd, K. Hong, S. Song, and H. Kuh, *J. Controlled Release*, 2010, **142**, 101.
- V. Sreekanth, S. Bansal, R. K. Motiani, S. Kundu, S. Muppu, T. D. Majumdar, K. Panjamurthy, S. Sengupta, and A. Bajaj, *Bioconjug. Chem.* 2013, **24**, 1468.